



OPEN ACCESS

EDITED BY

Lawrence H. Tanner,
Le Moyne College, United States

REVIEWED BY

Entao Liu,
China University of Geosciences (Wuhan),
China
Chao Fu,
China National Offshore Oil Corporation,
China

*CORRESPONDENCE

Youbin He,
✉ 100709@yangtzeu.edu.cn

RECEIVED 26 June 2023

ACCEPTED 04 September 2023

PUBLISHED 09 October 2023

CITATION

Feng B, He Y, Li H, Li T, Du X, Huang X and
Zhou X (2023), Paleogeographic
reconstruction of an ancient source-to-
sink system in a lacustrine basin from the
Paleogene Shahejie formation in the
Miaoxibei area (Bohai Bay basin,
east China).
Front. Earth Sci. 11:1247723.
doi: 10.3389/feart.2023.1247723

COPYRIGHT

© 2023 Feng, He, Li, Li, Du, Huang and
Zhou. This is an open-access article
distributed under the terms of the
[Creative Commons Attribution License
\(CC BY\)](https://creativecommons.org/licenses/by/4.0/). The use, distribution or
reproduction in other forums is
permitted, provided the original author(s)
and the copyright owner(s) are credited
and that the original publication in this
journal is cited, in accordance with
accepted academic practice. No use,
distribution or reproduction is permitted
which does not comply with these terms.

Paleogeographic reconstruction of an ancient source-to-sink system in a lacustrine basin from the Paleogene Shahejie formation in the Miaoxibei area (Bohai Bay basin, east China)

Bin Feng¹, Youbin He^{1*}, Hua Li¹, Tao Li¹, Xiaofeng Du²,
Xiaobo Huang³ and Xiaoguang Zhou³

¹School of Geosciences, Yangtze University, Wuhan, China, ²China National Offshore Oil Corporation, Beijing, China, ³Tianjin Branch of China National Offshore Oil Corporation, Tianjin, China

The paleogeographic reconstruction of ancient source-to-sink systems is a current focus and challenge in the field of Earth sciences; however, there are few established method or representative reconstruction case for ancient source-to-sink system paleogeographic reconstruction. Using drilling, thin-section, core, and 3D seismic data guided by sequence stratigraphy and sedimentology and the source-to-sink system approach, the source-to-sink system characteristics of the second member of the Paleogene Shahejie Formation in the Miaoxibei area of the Bohai Bay Basin were reconstructed. In addition, a new method for paleogeographic reconstruction of the ancient source-to-sink system was established using geomorphology and sediment backfilling technology to identify the erosion evolution history of the provenance area and to reconstruct the study area source-to-sink system for the investigated time-span. This study shows that a complete near-transport source-to-sink system developed in the Miaoxibei area, with the source area composed of Mesozoic granites, Neoproterozoic quartzites, and conglomerates. The primary and secondary watersheds were trending in N–S and E–W directions, respectively. The paleo drainage system trended in a N–S and E–W direction. The sedimentary facies represent mainly fan deltas and lakes. During the Paleogene, erosion was stronger in the western part of the source area than that in the eastern part, and the position of the paleo watershed gradually shifted eastward. The reconstruction method presented here and its results on the source-to-sink system can facilitate ancient source-to-sink system research in continental basins and serve as a model for paleogeographic reconstruction of ancient source-to-sink systems and related hydrocarbon exploration in other regions.

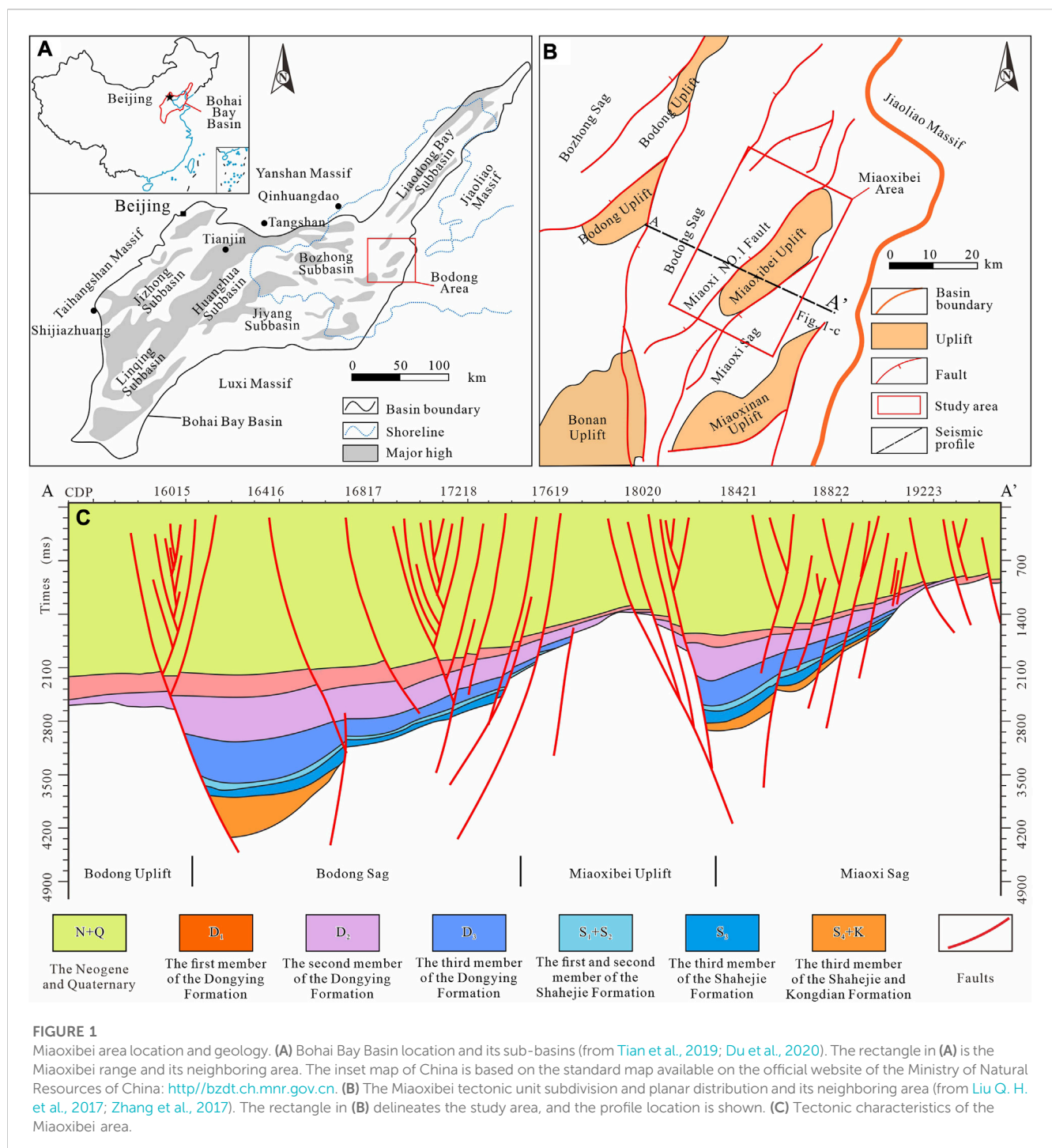
KEYWORDS

Bohai Bay basin, Miaoxibei area, paleogene, reconstruction, source-to-sink systems, sedimentology

1 Introduction

The source-to-sink system is one of the four main research fields proposed in the U.S. “MARGINS Program Science Plans 2004” (Li et al., 2003; Allen, 2005; 2008; Gao, 2005; Syvitski and Miliman, 2007; Wang, 2009; Martinsen et al., 2010; Liu E. T. et al., 2020) and is currently widely used in sedimentary research (Amorosi et al., 2016; Anderson et al., 2016; Walsh et al., 2016; Shao et al., 2019; Tian et al., 2019). In recent years, the study of source-to-sink systems in sedimentary basins has achieved a series of considerable results in driving response

mechanisms, quantitative relationship of elements, prediction of high-quality hydrocarbon source rocks and high-quality reservoirs, and reconstruction of ancient source-to-sink system. However, complex source rock types, tectonic evolution and paleogeomorphology, multi-directional sediment supply, and co-occurrence of various sedimentary systems make characterization more challenging (Xie and Li, 1993; Jiang, 2010; Weissmann et al., 2010; Fielding et al., 2012; Xu, 2013; Zhu et al., 2013; Lin et al., 2015; Liu H. et al., 2020; Liu et al., 2022). In addition, the reconstruction of ancient source-to-sink systems in lacustrine basins and continental basins is



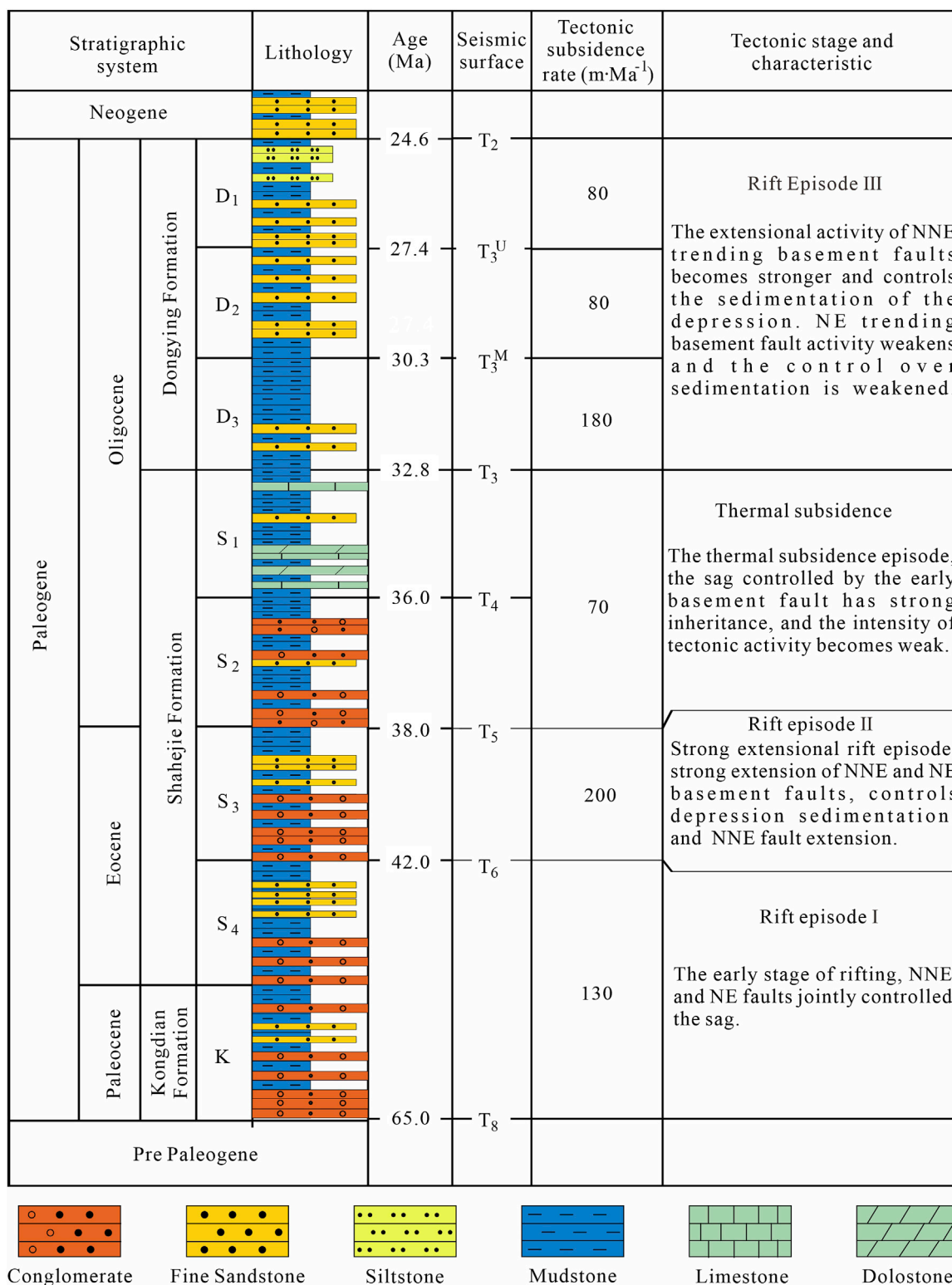


FIGURE 2 Miaoixibei area lithostratigraphy and strata pictorial chart. Lithological data and interpretations are based on a combination of data from wells located in the study area and neighboring regions (Tectonic date are modified from Li, 2015).

particularly challenging, given the limitations of the ancient geological record and the irreversibility of geological processes (Morehead, 1999; Romans et al., 2016; Shao et al., 2019). How to

reconstruct an ancient “Source-to-Sink” System in a Lacustrine Basin? Remains a current priority and challenge in the field of Earth sciences.

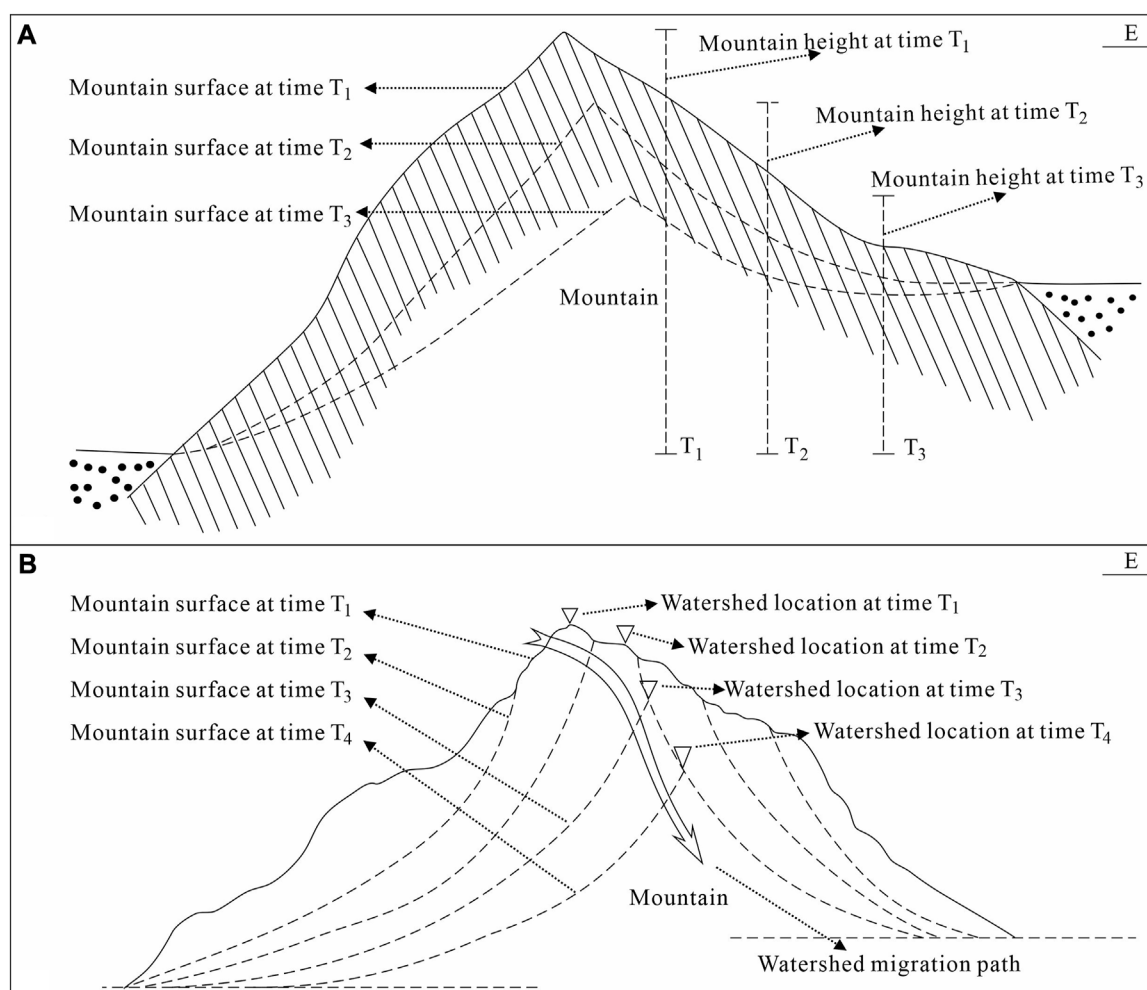


FIGURE 3

Erosion process schematic representation in the source area. (A) Reduction in source altitude. From time T1 to T3, the source altitude was reduced (modified from Yang L.Z, 1985). (B) Watershed migration from time T1 to time T4. The watershed migrated from west to east and from high to low (modified from South China Agricultural University, 1980).

The Miaoxibe area is located in the east of Bohai Bay Basin, one of the largest lacustrine basins in China. The Miaoxibe area is a well-developed Paleogene sequence with multiple sets of reservoir cap assemblages and successful hydrocarbon exploration (Wu et al., 2014; Figure 1A). However, to date, exploration of the Paleogene sequence has been relatively limited (Liu P. B et al., 2017; Zhu, 2020). Regarding the Miaoxibe area, the lack of sedimentary research is one of the main problems restricting hydrocarbon exploration (Sambrook Smith et al., 2010; Sømme et al., 2009; Sømme and Jackson, 2013; Liu Q. H et al., 2017). Therefore, it is necessary to describe the sedimentary system and reconstruct the paleogeographic source-to-sink system to guide the prediction of deeply buried layer sedimentary facies in the Miaoxibe area.

To address these issues and based on the study of the source-to-sink system characteristics in the second member of the Paleogene Shahejie Formation in the Miaoxibe area, a method for reconstructing the paleogeographic source-to-sink systems is proposed. The paleogeographic source-to-sink system of the second member of the Paleogene Shahejie Formation during the sedimentary period is

reconstructed. In this study, the distribution of deep-layer sedimentary systems could be predicted more accurately, and these findings have provided a sedimentary basis for hydrocarbon exploration. These findings also offer the potential to promote further research progress in continental basin source-to-sink systems and provide a scientific basis and case reference for studying source-to-sink systems in the Bohai Bay Basin and other areas with similar geological conditions.

2 Geological background

The Bohai Bay Basin, located in eastern China, is a lacustrine basin developed on top of the basement of the North China land mass, with an area of about 20×10^4 km² (Liu P. B et al., 2017; Zhu, 2020). The basin is bounded by the Taihangshan Uplift in the west, the Jiao-liao Uplift in the east, the Yanshan Uplift in the north, and the Luxi Uplift in the south, and can be divided into six depression tectonic zones, including the Linqing Depression, the Jizhong Depression, the Bohaizhong Depression, and the Liaodongwan

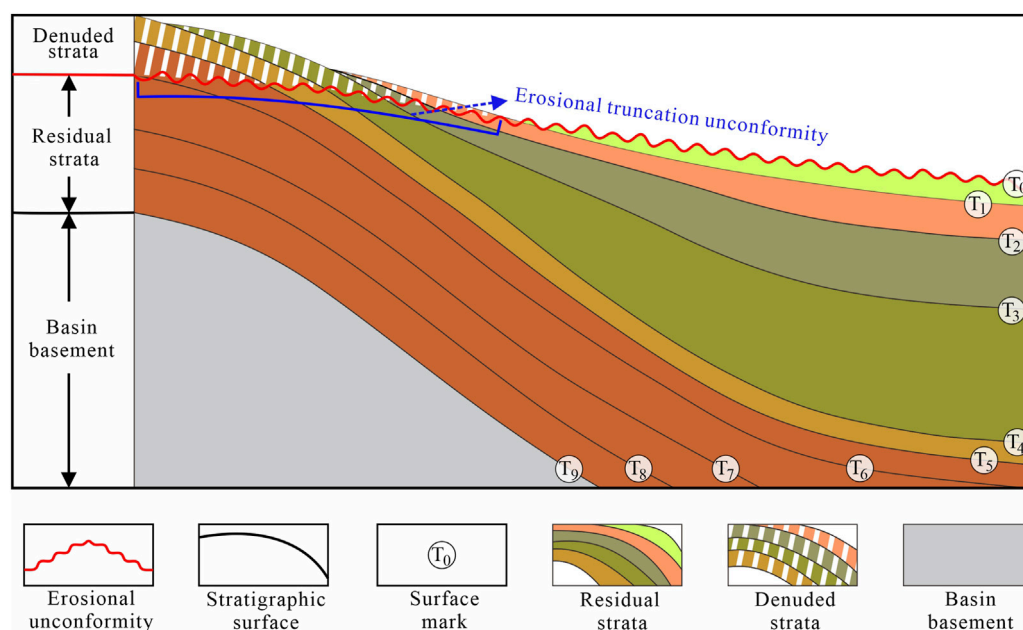


FIGURE 4

Schematic diagram representing the stratigraphic trend method, which recovers the denudation amount by using non-denuded strata structural and internal morphological characteristics. On the unconformity, surfaces T5 and T4 of the denuded strata refer to the underlying strata and extend from the equal thickness rule; surface T3 refers to T4 and the decreasing trend of residual strata thickness; surfaces T2 and T1 are similar to T3 and refer to the below surface.

Depression (Figure 1A). The Cenozoic of the Bohai Bay Basin is characterized by the superposition of multiple tectonic gyres and the composite of multiple orogenic mechanisms, and is filled with Paleoproterozoic fault tectonic systems and Neoproterozoic depression tectonic systems (Liu Q. H et al., 2017; Zhu, 2020).

The Miaoxibei area is located on the eastern edge of the Bohai Bay Basin in a sloping zone (Figure 1A). It comprises the Miaoxibei Uplift and the Bodong Sag, with an area of 442 km². The Miaoxibei Uplift is sandwiched between the Bodong and Miaoxi Sags and is controlled by the NE-SW trending half-anticline structure along the major fault (Miao No. 1 Fault) on the northeastern boundary (Figure 1B). The northwestern part of the Miaoxibei Uplift is deeper toward the northwest and gradually shallows to the southeast, exhibiting an asymmetric feature of west low and east high (Liu P. B et al., 2017; Zhang et al., 2017; Figure 1C).

Drilling data has shown that the Kongdian, Shahejie, and Dongying Formations of the Paleogene are developed in the Bodong Sag (Figure 2). The Shahejie Formation can be divided into four parts: the first, second, third, and fourth members of this formation. The target unit here is the second member of the Paleogene Shahejie Formation, which predominantly consists of a set of fan delta to lacustrine sediments. The main lithologies include conglomerate, sandstone, and mudstone, with a thickness of approximately 50–150 m (Li, 2015; Zhu, 2020).

The Paleogene tectonic evolution in the Miaoxibei area can be divided into rifting I stage of Kongdian Formation to the fourth Member of the Shahejie Formation, rifting II stage of the third Member of the Shahejie Formation, thermal subsidence stage of

the first and second Member of the Shahejie Formation, and rifting III stage of the Dongying Formation (Li, 2015; Figure 2). The sedimentary time-span of the second member of this formation was generally a thermal subsidence regime after a taphrogeny (Li, 2015; Figure 2). Tectonic movement predominantly occurred in the thermal subsidence, and the tectonic activity was weak, with the early period tectonic characteristics being inherited (the third member of the Shahejie Formation and Kongdian Formation), which preserved the Paleogene early period tectonic characteristics (Li, 2015). During the Paleogene, the Miaoxibei area exhibited a tectonic pattern of alternating uplift and depression, and the detritus from the Jiaoliao Uplift outside the Bohai Bay Basin is blocked by the Miaoxi Sag and Miaoxibei Uplift, and was not transported to the Bodong Sag (Li, 2015; Zhu, 2020). The Shahejie Formation shows strong inheritance of early period tectonic and sedimentary features during its sedimentation (Li, 2015). The Miaoxibei Uplift and Bodong Sag form a complete source-to-sink system (Zhu, 2020), providing suitable conditions for conducting sedimentological studies using a source-to-sink system approach. Therefore, the second member of the Shahejie Formation was selected as the target stratum for this study.

3 Research data and methods

Drilling and 3D seismic data from the entire Bodong area were collected by the China National Offshore Oil Corporation (CNOOC). There were a total of nine drill holes in the study area, among which Wells A-1, B-1, B-2, and C-1 encountered the

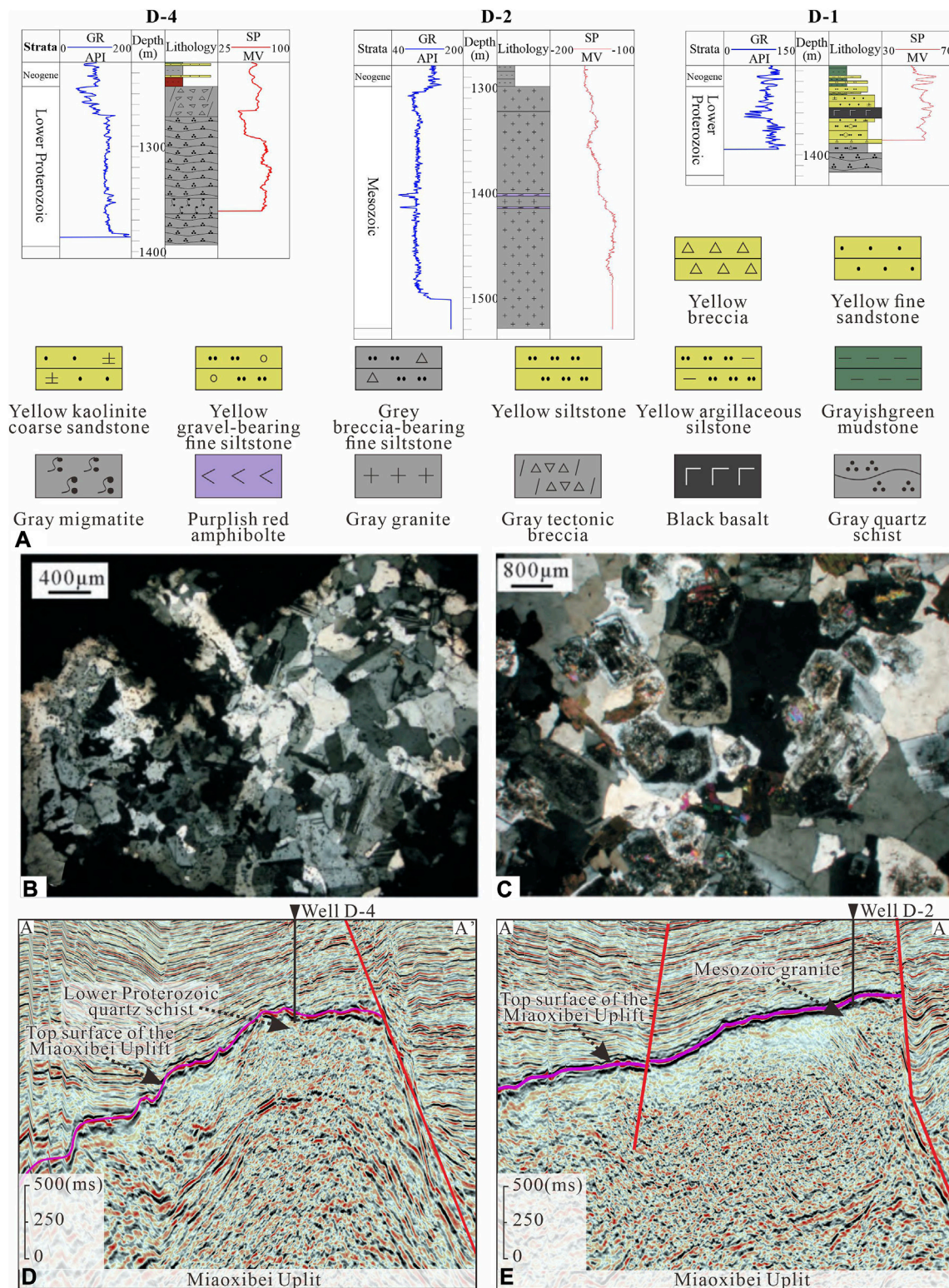


FIGURE 5 Sections and images showing bedrock lithology and geophysical characteristics in the Miaoxibei Uplift. **(A)** Miaoxibei Uplift bedrock well section. **(B)** Well D-2 thin section at a depth of 1,350 m, under cross-polarized light, revealing adamellite with a granite and monzonitic structure. The main minerals are quartz, potassium feldspar, plagioclase, biotite, and amphibole. **(C)** Well D-3 thin section at a depth of 1,365 m, under cross-polarized light, revealing granodiorite with hypidiomorphic granular texture and a red plaque indicating local potassic alteration. The main minerals are quartz, feldspar, plagioclase, hornblende, and biotite. **(D)** Well D-4 cross-well seismic profile. **(E)** Well D-2 cross-well seismic profile. Thin section data are cited from the literature. The location of the well connection section and seismic sections are marked in Figure 6.

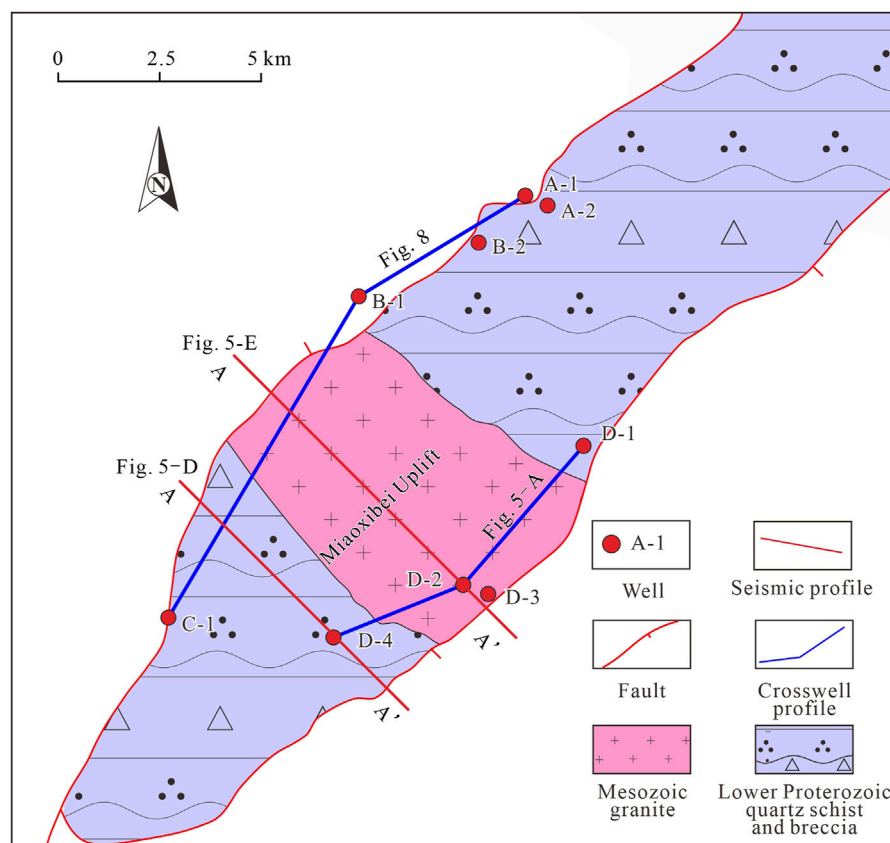


FIGURE 6

Schematic layout showing the bedrock lithology distribution in the Miaoxibei Uplift. The lithology in the Miaoxibei Uplift middle part is Mesozoic granite, and the southern and northern areas are Lower Proterozoic quartz schist and breccia.

second member of the Shahejie Formation. The main frequency of the seismic data is 32 Hz with an effective frequency range of 0–68 Hz. Detailed data including the lithologies (nine wells), well logs, sidewall cores (23 samples), and thin sections (27 samples) were also available for analysis in this study.

Relatively detailed methods have been developed for the elements of the source-to-sink system in continental basins, including bedrock types, watersheds, paleo rivers, transport pathways, sedimentary facies distribution, and paleogeomorphological features (Yang J. C., 1985; Liu et al., 2016; Zhao et al., 2017; Li et al., 2021; Zhao et al., 2021). Therefore, this study examined source-to-sink system paleogeographical reconstruction methods. This reconstruction comprises two parts, that is, paleogeographical reconstruction in the source and sedimentary areas (Shao et al., 2019).

3.1 Source area paleogeographical reconstruction method

Regarding the source area paleogeographical reconstruction, classical geomorphology theory highlights two important source erosion processes, namely, a) the decrease in source altitude (Figure 3A) (Yang L.Z., 1985), and b) the migration of the

watershed (Figure 3B; South China Agricultural University, 1980). Based on studies on erosion evolution models focusing on source area residual geomorphology and using the sediment backfilling method (Helland et al., 2016; Shao et al., 2019), the paleogeography of this area was reconstructed.

3.2 Sedimentary area paleogeographical reconstruction method

The methods for sedimentary strata reconstruction paleogeomorphology mainly include geophysical (Bai et al., 2002), imprinting (Xia and Ma, 1999), compaction thickness restoration (Jiang et al., 2009), residual thickness (He et al., 2007), and stratigraphic trend methods (Li et al., 2007). Among them, the imprinting method considers the influence of pre-sedimentary structures and can quantitatively represent paleogeomorphology. However, it cannot effectively restore denudation (Xia and Ma, 1999), whereas the stratigraphic trend method can accurately do this (Li et al., 2007; Figure 4). Therefore, in the continental basin, using the imprinting method combined with the stratigraphic trend method is more accurate for reconstructing sedimentary strata paleogeographical characteristics.

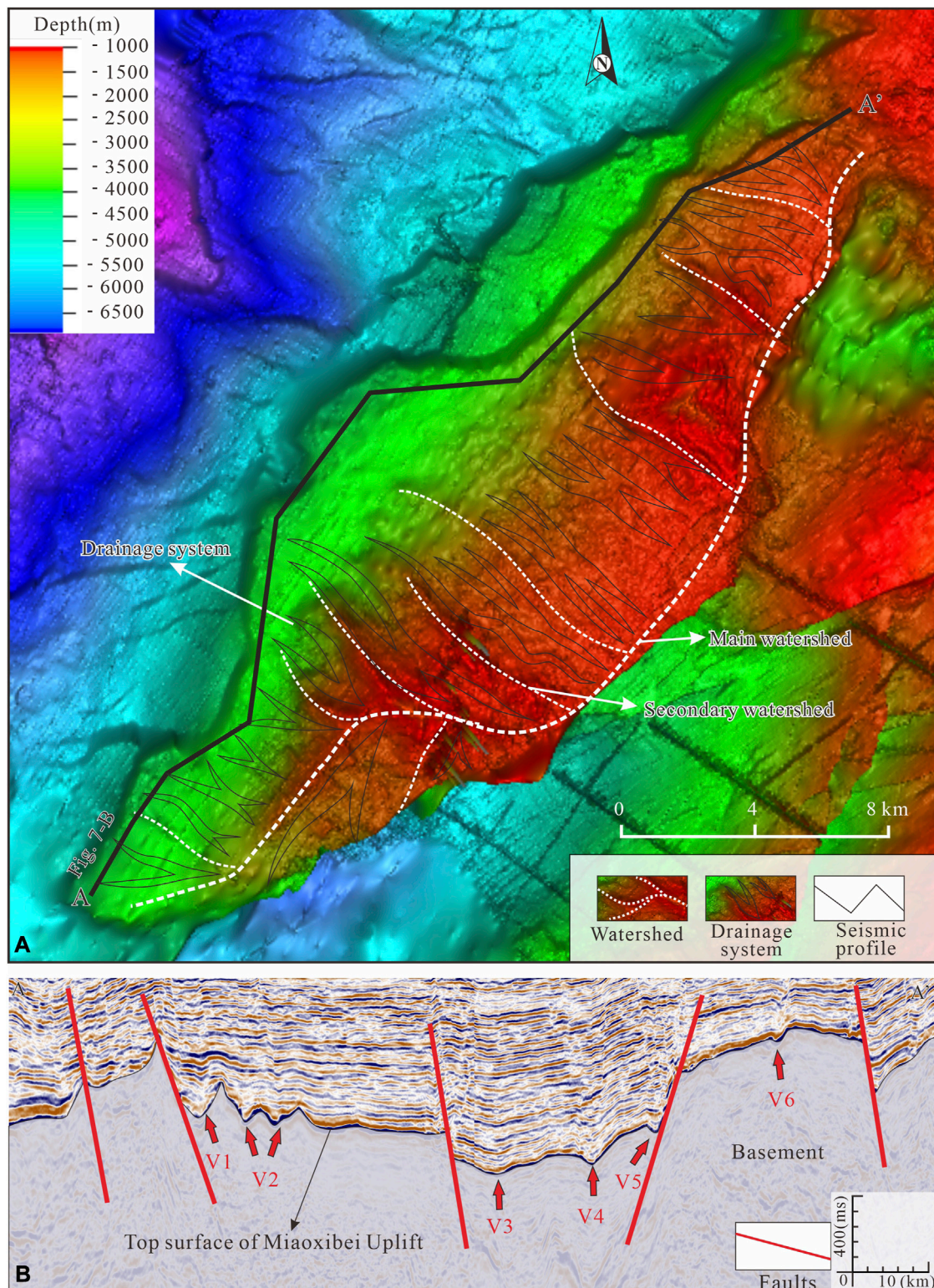
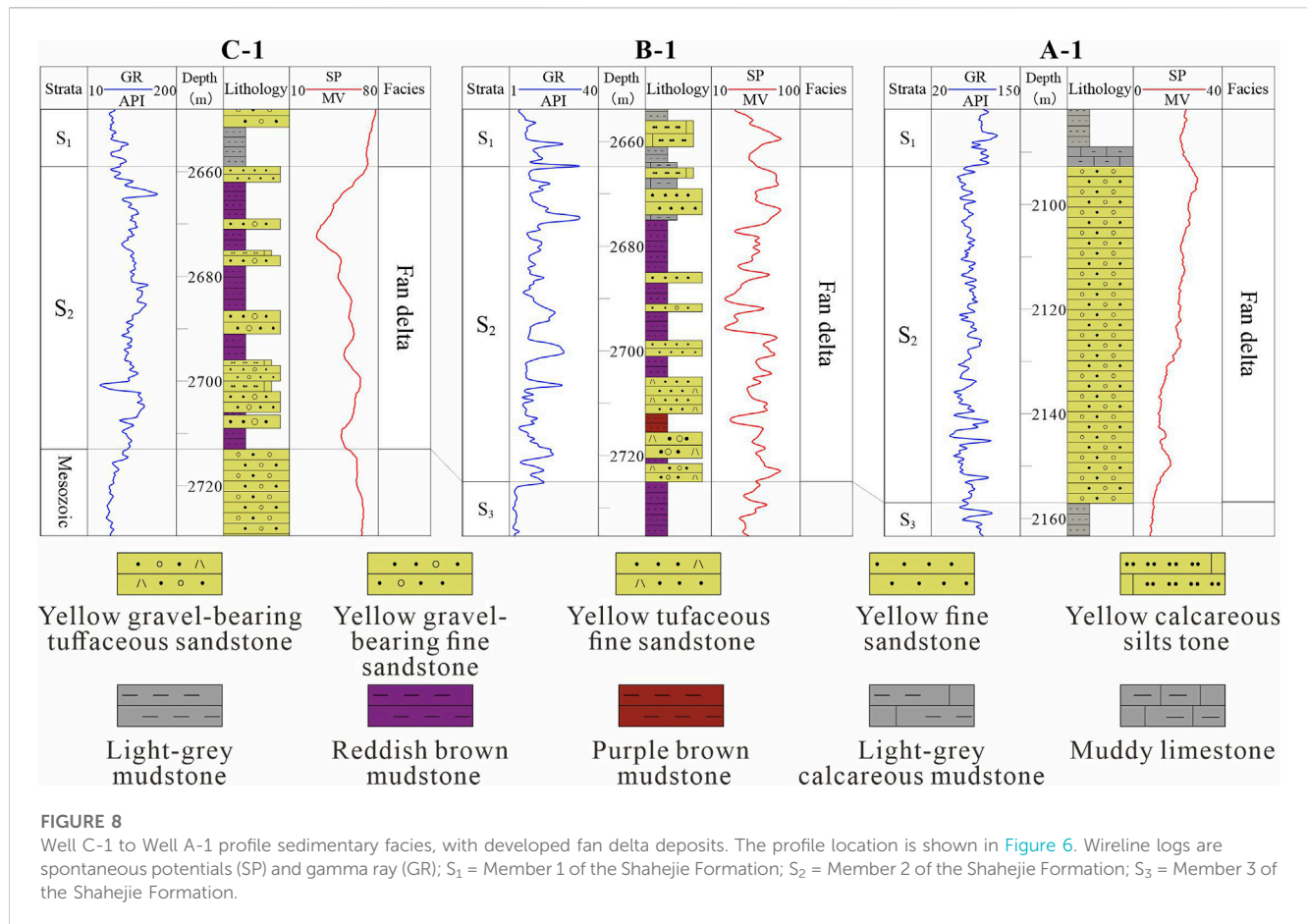


FIGURE 7

Digital elevation model (DEM) and seismic profile images depicting the Miaoxibei Uplift geomorphic characteristics, paleo watershed, drainage system distribution, and transport pathway characteristics. **(A)** Watershed and drainage system distribution in the Miaoxibei Uplift. The base map is the top structure map of the Miaoxibei Uplift. **(B)** Transport pathway seismic characteristics. Red arrows mark the transport pathway development position, and the profile location is shown in **(A)**.



4 Source-to-sink system characteristics

4.1 Source characteristics

4.1.1 Source lithology

Drilling data suggest that the Miaoxibei Uplift bedrock consists of Mesozoic granite and Early Proterozoic quartz schist. Well D-4 predominantly consists of Early Proterozoic quartzite and conglomerate. The main lithology of Well D-2 is Mesozoic granite, with conglomerate at the top. The bottom of Well D-1 is Lower Proterozoic quartzite, gradually changing to include conglomerate, fine sandstone, and siltstone at the top (Figure 5A).

Thin sections of Wells D-3 and B-1 in the Miaoxibei Uplift showed that the Mesozoic granite is mainly granodiorite, with a small proportion of biotite granite. Thin section data from Well D-3 showed that its lithology was gray-white blocky granite (Figure 5B). The main mineral components were quartz, potassium feldspar, plagioclase, biotite, and hornblende. Thin section data from Well D-2 showed that its lithology is gray-white blocky granodiorite with a semi-self-shaped granular structure, with local potassium alteration shown as reddish patches (Figure 5C). The main mineral components were quartz, potassium feldspar, plagioclase, hornblende, and biotite (Zhao et al., 2017).

The seismic reflections of Mesozoic granite, Lower Proterozoic quartzite, and conglomerate are distinct. Lower

Proterozoic quartzite and conglomerate showed weak-amplitude, low-frequency, intermittent worm-like reflective seismic phases (Figure 5D). The Mesozoic granite displayed medium-strong amplitude and medium-high frequency chaotic reflective seismic phases (Figure 5E). Based on this, the boundary and lithology distribution of the Miaoxibei Uplift were determined. Lower Proterozoic quartzite and conglomerate were distributed in the north and south sides of the Miaoxibei Uplift, and Mesozoic granite is distributed in the center (Figure 6).

4.1.2 Watershed and drainage system

Under the action of differential denudation, a series of high points and channels are formed on the top surface of the Miaoxibei Uplift. According to the structural characteristics and trend of the Miaoxibei Uplift, the connection of the series of high points is the watershed, and the combination of a series of channels from high to low and from upstream to downstream is the drainage system (Liu Q.H et al., 2017; Zhu, 2020). Based on the watershed development scale, the Miaoxibei Uplift watershed can be divided into main and secondary watersheds (Figure 7A). The main watershed runs north-south along the long axis of the Miaoxibei Uplift, usually closer to the southeastern side. The secondary watersheds are scattered on the Miaoxibei Uplift along the short axis, intersecting perpendicularly or at acute angles to the main watershed. Due to the influence of the watersheds, the drainage systems in the southern and northern parts were small in scale but

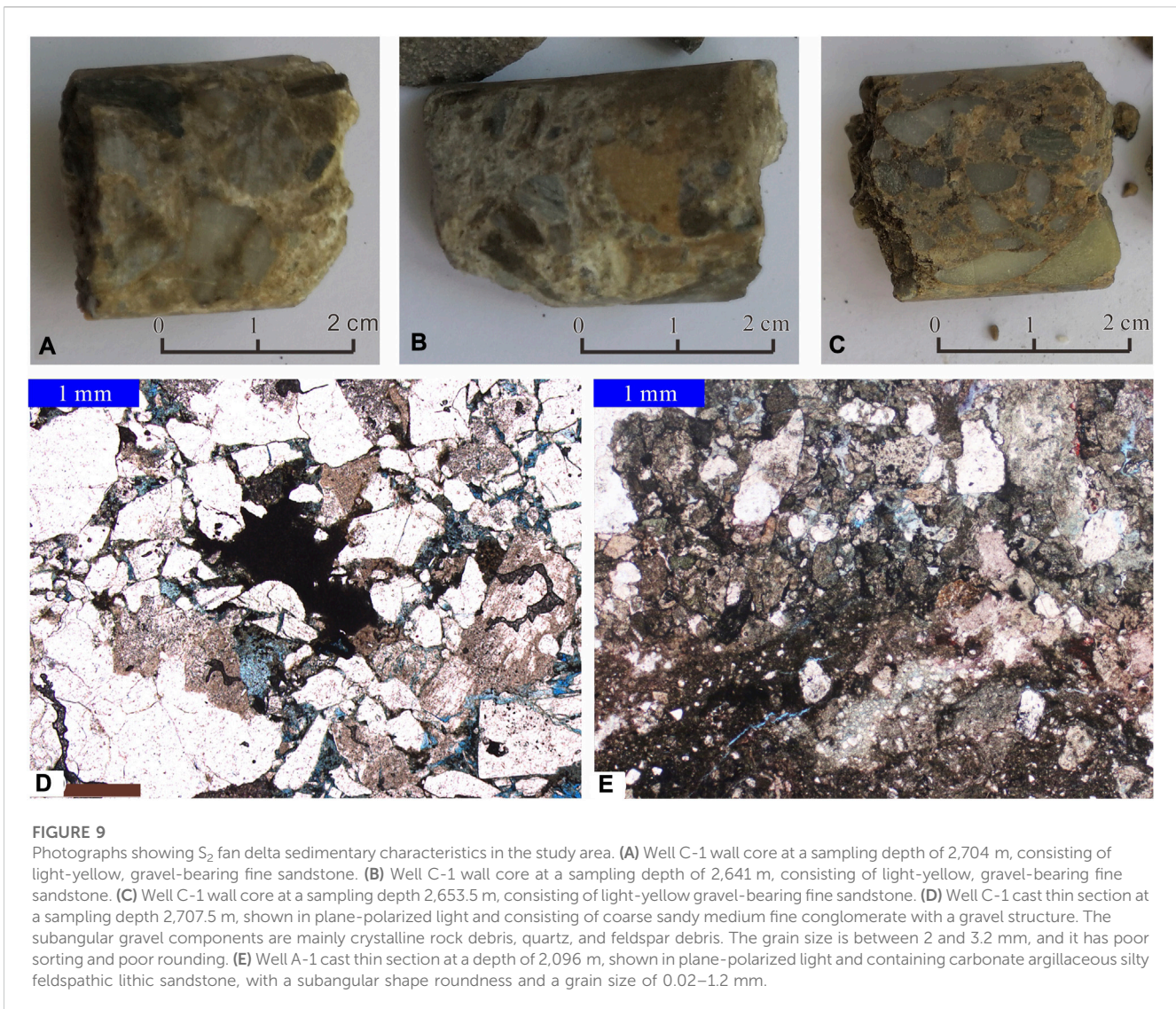


FIGURE 9

Photographs showing S_2 fan delta sedimentary characteristics in the study area. (A) Well C-1 wall core at a sampling depth of 2,704 m, consisting of light-yellow, gravel-bearing fine sandstone. (B) Well C-1 wall core at a sampling depth of 2,641 m, consisting of light-yellow, gravel-bearing fine sandstone. (C) Well C-1 wall core at a sampling depth 2,653.5 m, consisting of light-yellow gravel-bearing fine sandstone. (D) Well C-1 cast thin section at a sampling depth 2,707.5 m, shown in plane-polarized light and consisting of coarse sandy medium fine conglomerate with a gravel structure. The subangular gravel components are mainly crystalline rock debris, quartz, and feldspar debris. The grain size is between 2 and 3.2 mm, and it has poor sorting and poor rounding. (E) Well A-1 cast thin section at a depth of 2,096 m, shown in plane-polarized light and containing carbonate argillaceous silty feldspathic lithic sandstone, with a subangular shape roundness and a grain size of 0.02–1.2 mm.

large in quantity, while those in the central part were large in scale but small in quantity.

4.2 Transport pathway characteristics

The sediment transport on the Miaoxibei Uplift followed valleys, which can divide into V-shaped, U-shaped, and compound valleys, as well as single fault type troughs (Figure 7B). V1, V2, V3, V4, V5, and V6 were single fault troughs, compound valleys, U-shaped, V-shaped, single fault troughs, and V-shaped, respectively.

4.3 Sedimentary facies

Based on drilling, thin-section, core, and seismic data, it was found the sediments under study represent fan deltas and lakes.

Fan deltas are composed of conglomeratic sandstone, fine sandstone, and mudstone, and their logging characteristics are

dominated by a toothed bell shape and funnel shape (Figure 8). Wall-core data from the second member of the Shahejie Formation of Well C-1 indicated that it consists of light-yellow, gravel-bearing fine sandstone that is poorly sorted and rounded (Figures 9A–C).

Thin-section data from a depth of 2,707.5 m in the second member of Well C-1 showed that it contained coarse sandstone with fine gravel, which is poorly sorted and rounded (Figure 9D). The composition of clastic particles is 85%, the content of matrix is 5%, and the content of cement is 7%. The particle composition includes quartz, debris, feldspar, and a small amount of mica. The gravel and debris are mainly quartzite, shallow-grained rock, tuff, and granite.

Thin-section data from a depth of 2,096 m in the second member of Well A-1 showed that it is composed of carbonate containing argillaceous silty feldspathic lithic sandstone, with a particle size ranging from 0.02 to 1.2 mm and a high clay content (Figure 9E). The clastic particle composition is 79%, the matrix content is 7%, and the cement content is 9%. The gravel and rock debris are mainly quartzite, shallow grained rock, tuff, and

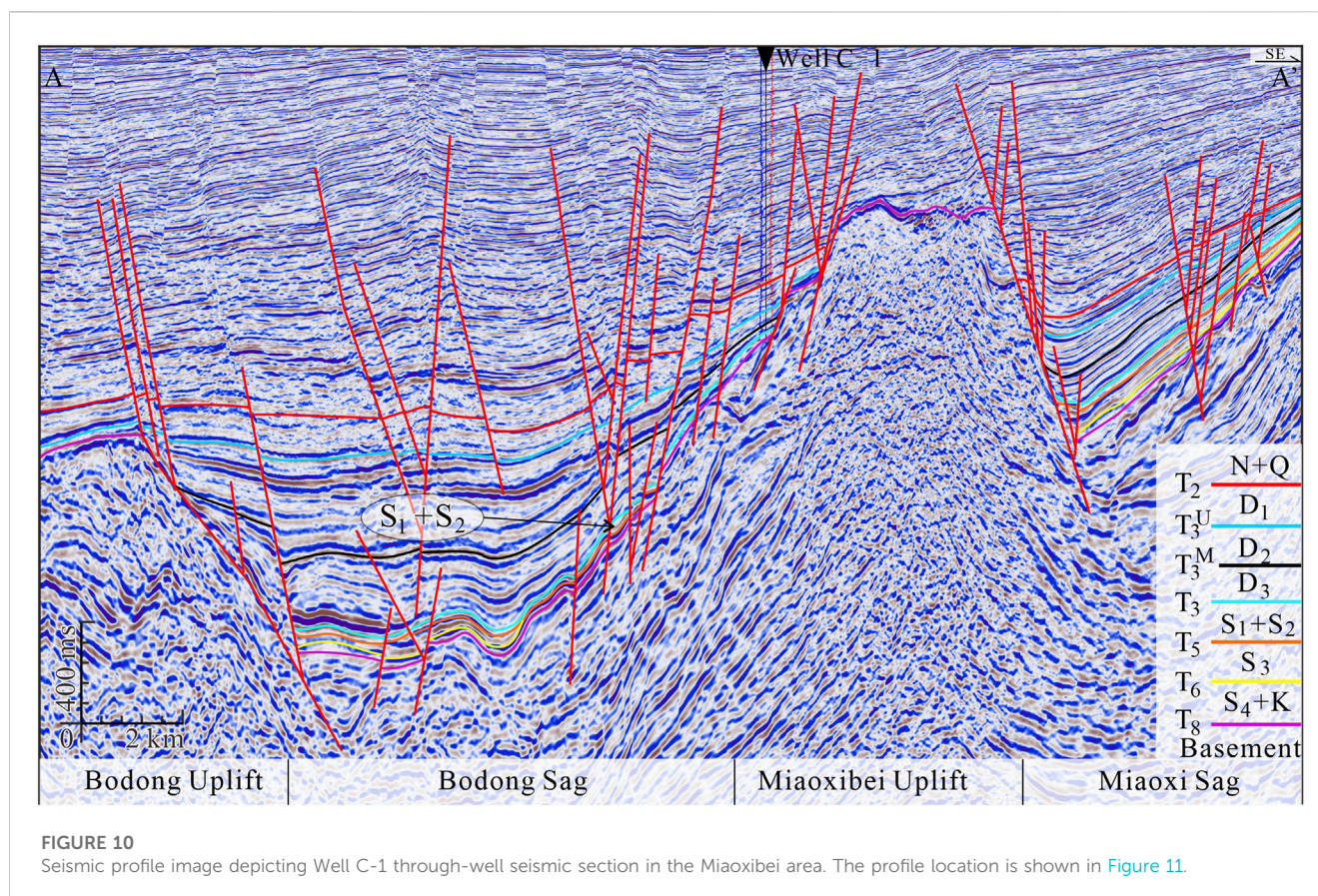


FIGURE 10

Seismic profile image depicting Well C-1 through-well seismic section in the Miaoxibei area. The profile location is shown in Figure 11.

metamorphic granite (Figure 9E). Thin section data show that the composition and mineral association of sandstone in the second member of the Shahejie Formation are well matched with quartz schist and granite in the Miaoxibei Uplift, and the sorting and roundness are bad, indicating that its source is from the Miaoxibei Uplift, the transport distance is relatively close and the accumulation rate is fast.

Given the relatively limited thickness layer of the second member (less than 50 ms and 50 m in the seismic and Well data, respectively), it appeared as a group of low-to-mid-frequency reflection phase axes in the seismic profile. This made it difficult to determine its external geometry and internal reflection structures (Figure 10). Therefore, the fan delta facies could only be distinguished from the shallow lake facies based on their seismic amplitude and continuity, which were characterized by medium to strong amplitude reflections and moderate to poor continuity. The drilling data showed that the mean amplitude seismic attribute of the second member had a strong response to the fan delta sedimentation and could be identified reliably (Figure 11).

Logging data calibration of the seismic attributes (average amplitude value) of the second member showed that fan deltas feature an abnormally high amplitude (red and yellow areas) (Figure 11A). This indicated their planar distribution, which varied considerably, with isolated buds as the main type in the south and strip-like, vertically aligned longitudinal axes trending toward north-northwest in the north. The middle fan developed at a large scale, gradually decreasing toward both sides (Figures 11A, B).

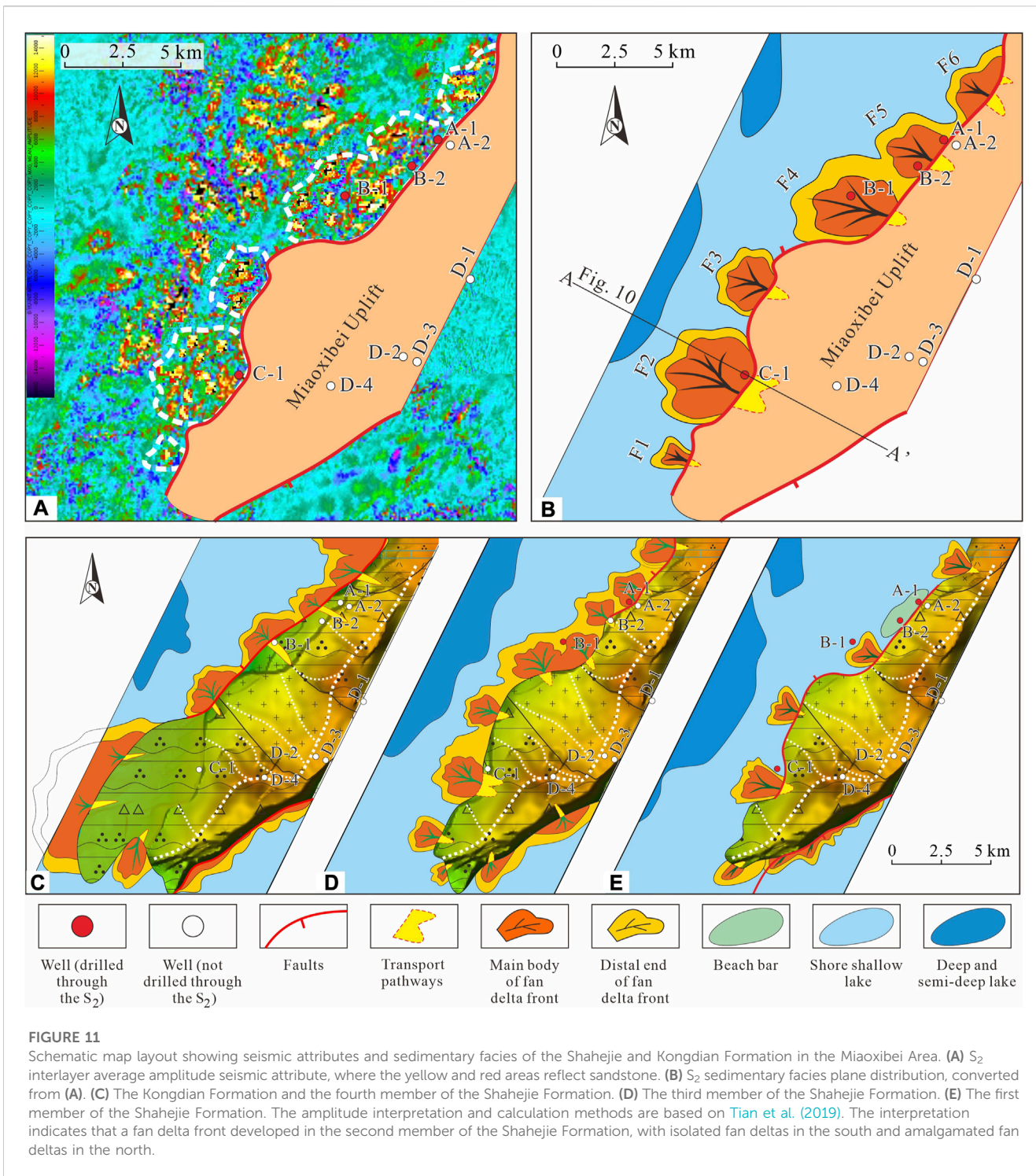
5 Source-to-sink system paleogeographical reconstruction

5.1 Depositional area

Seismic data indicated that in the southern part of the study area, the second member of the Shahejie Formation was predominantly controlled by faults with large displacement, and formation margin erosion was weak (Figure 10), resulting in relatively well-preserved stratigraphic boundaries. In the north of the study area, the fault displacement was relatively small, and formation margin erosion was relatively strong, resulting in relatively bad-preserved stratigraphic boundaries. Based on the paleogeomorphological reconstruction results, the thickness of the second member of the Shahejie Formation in Bodong Sag is between 50 and 150 m, and it is thinner in the east, thicker in the west, thinner in the south, thicker in the north, and the depositional center is in the north, the erosion in the northern part was relatively strong, and the eroded strata extended farthest toward the east at 4.8 km (Figures 12A, B).

5.2 Source area

The Miaoxibei Uplift top surface geomorphological characteristics indicated that the slopes on the eastern and western sides of the main watershed are asymmetric (Figure 7A). According to modern geomorphological theory, several factors can cause slope asymmetry on either side of watersheds, such as the



influence of geological structures and asymmetrical erosion at the base level and differences in rock properties or faults.

The study area structural characteristics suggested that the Miaoxibei Uplift western slope is gentle and belongs to the Bodong Sag gentle slope zone. In contrast, the eastern slope is steeper and belongs to the Miaoxi Sag steep slope zone (Figure 10). This indicates that the slopes on the Miaoxibei Uplift eastern and western sides may have been asymmetrical during the Bodong Sag rift stage.

The characteristics and scale of sedimentary filling (Figures 10, 11) indicate that the Paleogene strata in the Bodong Sag have a greater thickness and wider spatial distribution range compared with those in the Miaoxi Sag, which were thinner with a narrower spatial distribution range. In terms of the material conservation of the source-to-sink system, this suggests that during the Paleogene, erosion on the two sides of the Miaoxibei Uplift was uneven, with the western side experiencing stronger erosion than the eastern side. The

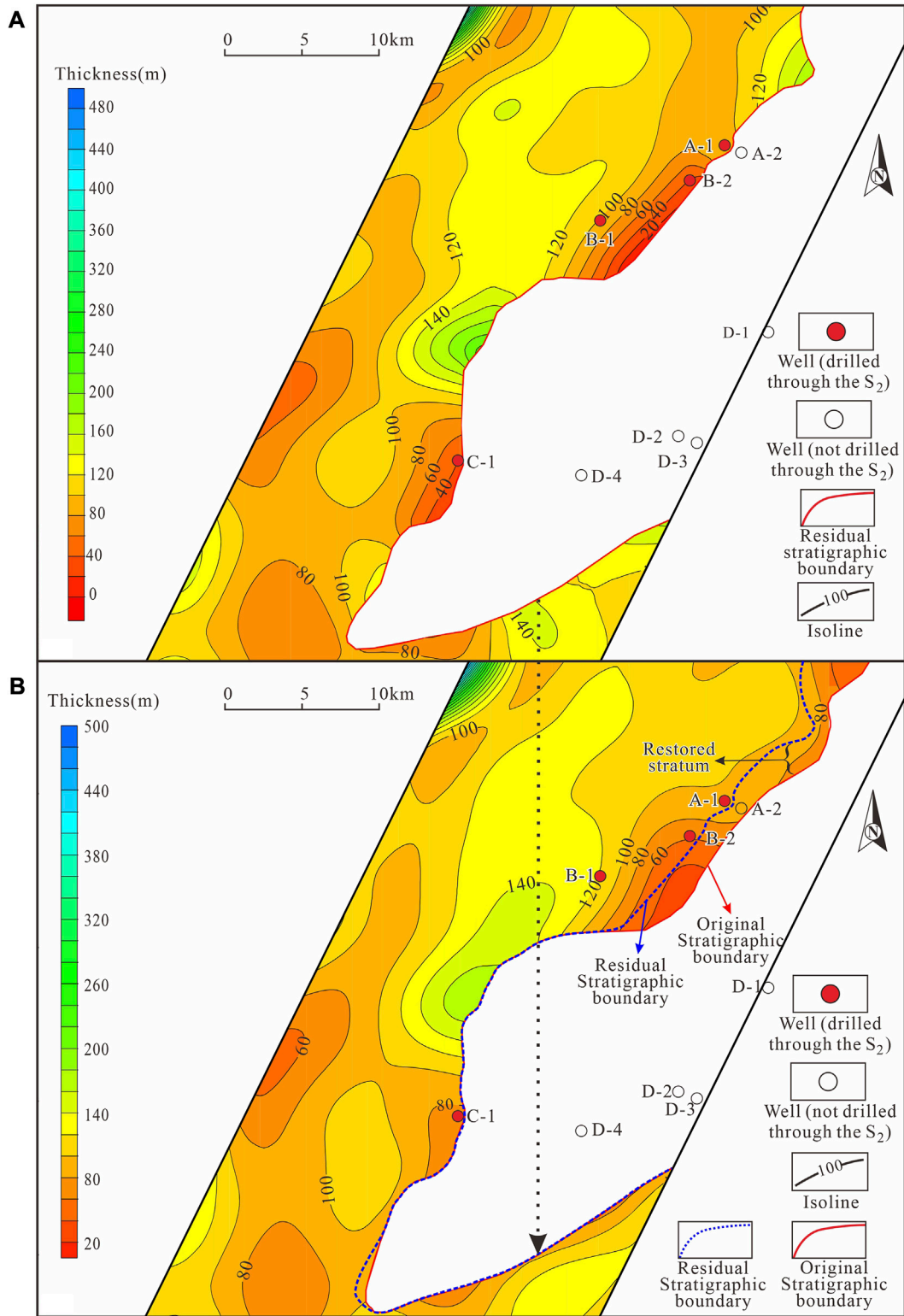


FIGURE 12

Contour map depicting residual and original thicknesses of the second member of the Shahejie Formation in the study area. **(A)** Residual thickness of the second member of the Shahejie Formation. **(B)** Original thickness of the second member of the Shahejie Formation. The blue dotted line represents the residual stratigraphic boundary, transplanted from **(A)**. The restored stratum is the area clamped by the residual and original stratigraphic boundaries.

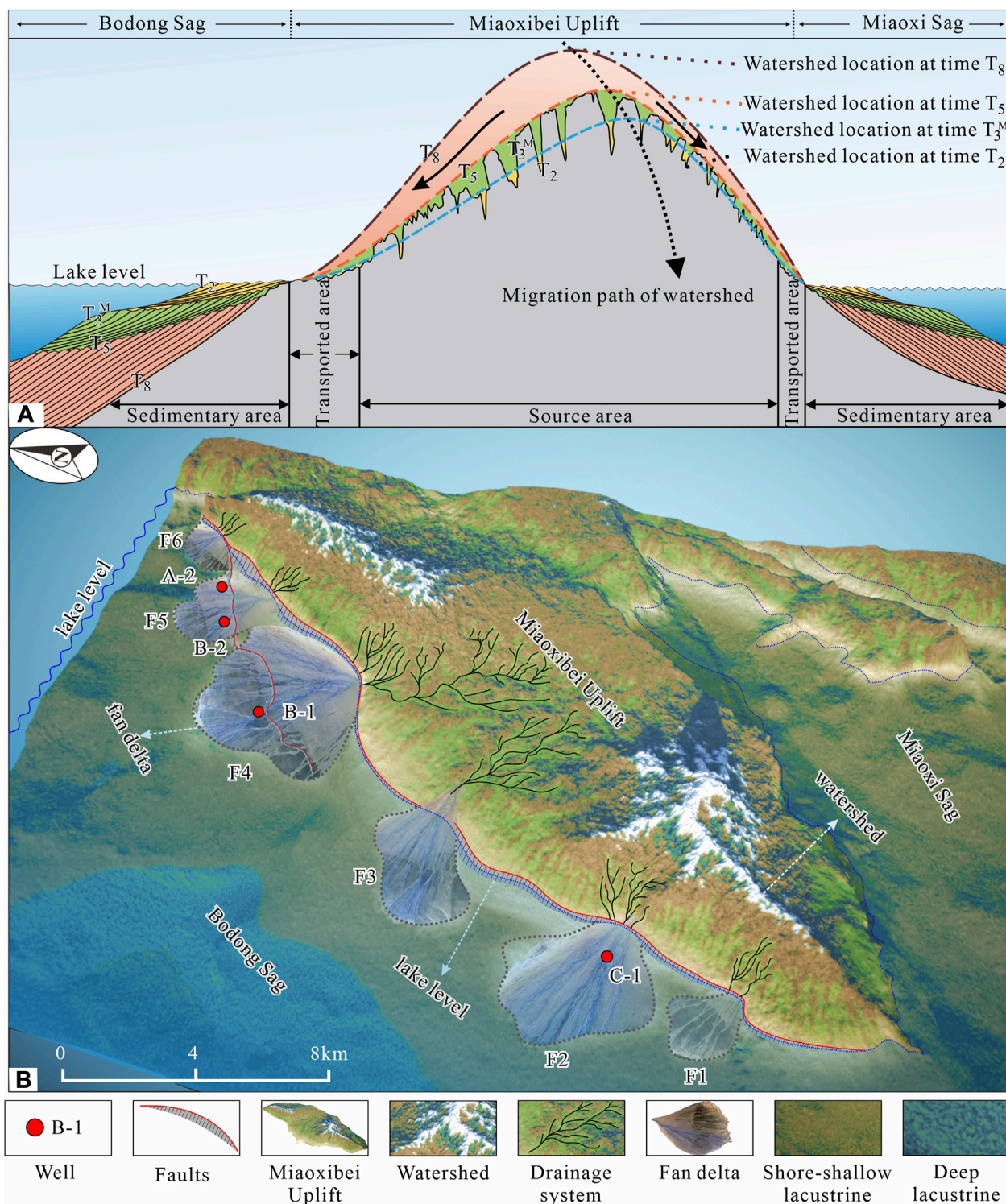


FIGURE 13

Schematic diagram and spatial image illustrating the Miaoxibei Area source-to-sink system reconstruction process and results. **(A)** The reconstruction process for source paleogeomorphology in the Miaoxibei Uplift and paleo watershed migration path. The original section is shown in Figure 10. From time T3 to T0, the paleo watershed migrated from west to east, and the reconstruction methods were derived from the literature (South China Agricultural University, 1980; Yang J. C., 1985; Helland et al., 2016). **(B)** The source-to-sink system paleogeographic reconstruction results in the Miaoxibei area. The north and south flanks of the uplift are high, the slope is steep, and the middle part is relatively gentle. The main watershed is distributed along the west side of the uplift long axis. The secondary watershed is distributed along the east–west direction, and the drainage system is scattered within the watersheds. The transport pathways and fan deltas correspond well, primarily developing isolated flower-shaped or continuous flower-shaped fan delta deposits. Large fan deltas developed in the northern and southern areas, with small fan deltas developing in the middle area.

TABLE 1 Statistical table of source-to-sink system elements of the second member of shahejie formation in the study area.

Number	Source system				Transport system				Sink system		
	Source			Drainage	Transport pathway				Fan delta		
	Area	Altitude	Volume	Length	Length	Width	Width-depth ratio	Sectional area	Area	Average thickness	Volume
	km ²	km	km ³	km	km	km	%	km ²	km ²	km	km ³
F1	18.8	1.6	15.04	4.3	0.87	0.35	2.5	0.24	10.4	0.05	0.52
F2	28.4	2.6	36.92	5.2	2.14	0.28	7.6	0.51	73.8	0.07	5.1
F3	56.4	2.9	81.78	8.3	2.52	0.26	9.7	0.32	31.3	0.07	2.3
F4	178.2	2.6	231.66	5.1	1.98	0.29	6.8	0.34	79.35	0.08	6.8
F5	129.6	2.2	142.56	6.2	0.63	0.18	3.5	0.05	48.8	0.06	3.3
F6	135.6	1.2	81.36	2.1	0.54	0.12	4.5	0.02	34	0.07	2.4

main watershed gradually shifted to the east under the influence of uneven and asymmetrical erosion at the base level.

Based on this, the Miaoxibei Uplift erosion process was traced back by analyzing a series of seismic profiles (Figure 10). During the Paleogene, the main watershed position migrated from west to east (Figure 13A). Under the watershed migration pattern constraint, the Miaoxibei Uplift paleogeomorphological reconstruction was completed (Figure 13B). Based on paleogeomorphology reconstruction and under the constraints of geomorphology, the drainage system above the source of the study area was reproduced by means of digital differential erosion simulation and three-dimensional proportional fluid simulation, and the drainage system corresponding to the fan delta in the study area was picked up and combined (Figure 13B). The drainage system in the middle part of the Miaoxibei Uplift was larger in scale, extended longer and had more tributaries. The drainage systems in the south and north are smaller in scale, with shorter distances and fewer tributaries.

Based on paleogeomorphology reconstruction and under the constraints of geomorphology, the drainage system above the source of the study area is reproduced by means of digital differential erosion simulation and three-dimensional proportional fluid simulation, and the main drainage system corresponding to the fan delta in the study area is picked up and combined in the form of lines (Figure 13B). The ancient water system in the central part of the temple northwest bulge is larger in scale, longer in extension distance and more tributaries, while it is smaller in the south and north with shorter in extension distance and fewer tributaries.

5.3 Reconstruction results

Based on the paleogeomorphological reconstruction in the sedimentary area and the sedimentary system distribution, as well as the paleogeomorphological reconstruction in the source area, the source-to-sink system of the second member of the Shahejie Formation in the Miaoxibei area was reconstructed (Figure 13B). The results show that the Miaoxibei Uplift northern and southern sides comprise large areas with high

altitudes and a strong sediment supply capacity. The Miaoxibei Uplift main watershed gradually shifted to the east during the Paleogene, and the transport pathways corresponded well to the fan deltas. The study area southern part is dominated by isolated fan deltas, while the northern part is dominated by continuous fan deltas, with a larger scale in the central area and a smaller scale on the northern and southern sides.

5.4 Relationship between the elements of the source-to-sink system

According to the reconstruction results, the sources in the southern and northern parts of the study area comprise a large area at high altitude, resulting in large-scale fan delta development (Figure 13B). During the sedimentation period of the second member of the Shahejie Formation, the tectonic activity was mainly thermal subsidence and weak (Figure 2), with a relatively small influence on the source-to-sink system process. The bedrock types in the Miaoxibei Uplift were mainly granite and quartzite, and modern geomorphic research shows that their resistance to weathering is similar (Yu et al., 2013). Therefore, we can rule out the influence of strong tectonic movement and provenance lithology difference on the development scale of fan delta in the study area.

Based on the reconstructed results, the parameters of various source-to-sink systems in the study area are quantitatively calculated by the method of calculus (Amorosi et al., 2016; Liu E. T. et al., 2020) (Table 1), and the correlations among the elements of various source-to-sink systems are analyzed.

The correlation analysis results of the height of the source, area of the source, volume of the source, length of the drainage system, and the cross-sectional area of the transport pathway show that (Figures 14A–D), the coefficient of determination (R^2) of the volume of the source, area of the source, length of the drainage system, and cross-sectional area of the transport channel are all less than 0.5, in which the coefficient of determination of height of the source and the cross-sectional area of the transport channel is relatively high, and the R^2 is 0.447. The cross-sectional area of the transport channel has low

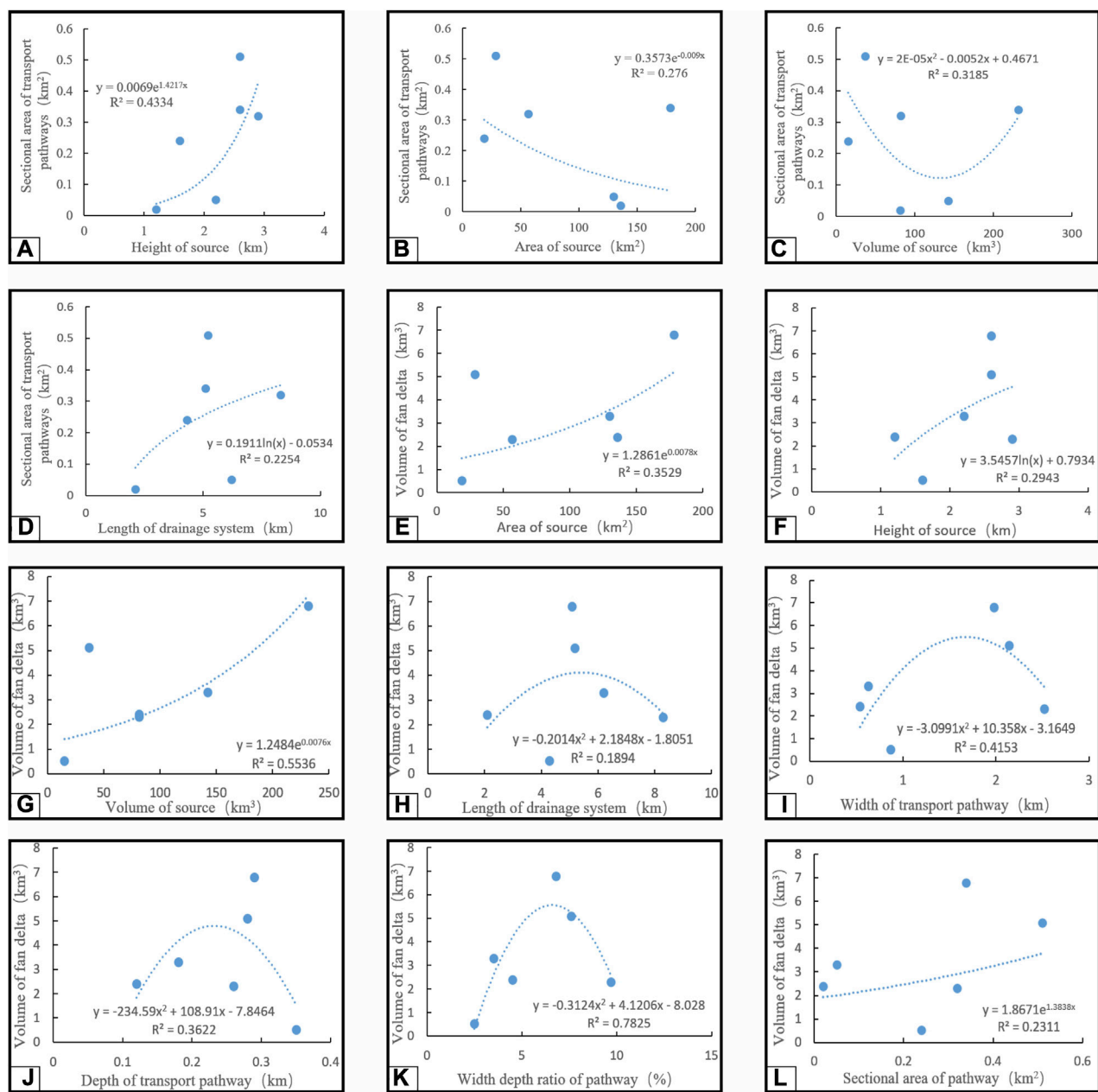


FIGURE 14

Relationships between the Elements of Source-to-Sink System. (A) Relationships between sectional area of transport pathway and height of source. (B) Relationships between sectional area of transport pathway and area of source. (C) Relationships between sectional area of transport pathway and volume of source. (D) Relationships between sectional area of transport pathway and length of drainage system. (E) Relationships between Volume of fan delta and area of source. (F) Relationships between volume of fan delta and Height of source. (G) Relationships between Volume of fan delta and volume of source. (H) Relationships between Volume of fan delta and length of drainage system. (I) Relationships between Volume of fan delta and width of transport pathway. (J) Relationships between Volume of fan delta and depth of transport pathway. (K) Relationships between Volume of fan delta and width depth ratio of transport pathway. (L) Relationships between Volume of fan delta and sectional area of transport pathway. Input data regarding the source-to sink parameters data are from Table 1. Regression-line equans and coefficients of determination (R^2) are shown for all diagrams.

correlation with the length of the drainage system, area of the source, and the volume of the source.

According to the correlation analysis results of the area of the source, height of the source, volume of the source, length of the drainage system, width of the transport pathway, depth of the transport pathway, width to depth ratio of the transport pathway, channel cross-sectional area of transport pathway, and volume of the

delta (Figures 14D–K), the volume of the source, width depth ratio of the transport pathway, and the volume of the delta have the strongest correlation, and the coefficient of determination (R^2) are 0.55 and 0.78. The correlation between the area of the source, height of the source, depth of the transport pathway, width of the transport pathway, channel cross-sectional area of transport pathway, and volume of the delta is low, and the correlation is power function or

polynomial, and the coefficient of determination (R^2) is between 0.3 and 0.4. The coefficient of determination (R^2) of length of the drainage system and the volume of the delta is less than 0.2, and there is no obvious correlation between them.

6 Discussion

6.1 Correlation between elements of source-to-sink system

In the study area, the volume of fan delta has a strong correlation with the volume of the source and the width depth ratio of the transport channel, but a weak correlation with the height of the source, area of the source, and the length of drainage system (Figure 14).

From the essence of “conservation of matter” in the “source-to-sink” system, the amount of denudation produced in the source directly determines the size of the delta volume (Xie et al., 2014; Helland et al., 2016; Zeng et al., 2019). Therefore, the delta volume should be the total amount of debris, which depends on the area of denudation, bedrock lithology, geomorphological characteristics, tectonic activity, and weathering intensity in the basin, independent of the transport distance and mode. This well explains the phenomenon in this study that the volume of delta is not obviously related to the transport distance, but is related to the volume of the source.

It is worth mentioning that the width depth ratio of the transport pathway in the study area has a strong correlation with the volume of fan delta, but too large or too small width depth ratio of transport pathway is not conducive to the large-scale development of delta. This phenomenon can be well explained in the theory of erosion cycle proposed by Davis in the middle of 18th century. The width depth ratio of the early development stage of the transport pathway is small, and the sediment flux is also small. In the middle stage, the ratio of width depth ratio was moderate and the deposition flux was maximum. In the late stage, the width depth ratio is larger and the deposition flux was smaller. A similar phenomenon has been reported in the case study of the “source-to-sink” system in the Bozhong Sag, where the width depth ratio of the transport pathway that is too large or too small is not always beneficial for delta enrichment (Zhou et al., 2017).

6.2 Significance for high-quality reservoir exploration

In areas where there has been relatively little exploration, traditional sedimentary facies research methods are predominantly based on well-log data to mark various geophysical features (Liu et al., 2016; Zhu et al., 2016; Ge et al., 2020; Zhao et al., 2021). The source-to-sink technique works effectively when well-log data is limited (Martinsen et al., 2005; Liu et al., 2019; Lin et al., 2022; Sambrook Smith et al., 2010; Sømme et al., 2009; Sømme and Jackson, 2013; Xu and Du, 2017; Xu et al., 2021; Zhou et al., 2017; Zhu et al., 2014; Zhu et al., 2017). Considering the Miaoxibe area as an example, the sedimentary

facies of the second member of the Shahejie Formation have been determined using well-log data and seismic attributes (Figure 11), it was found that transport pathways and fan deltas corresponded more effectively in the study area (Figure 14B). Transport pathways, such as valleys and fault troughs on top of the bedrock, are inheritable and their positions do not change considerably (Yang J. C., 1985; Li, 1999). With a lack of drilling data, this indicates that in the middle and deep layers of the third and fourth members of the Shahejie and Kongdian Formations, the transport channel may also strongly correspond with the fan deltas. This approach can be used to replace drilling data for calibrating geophysical data identifying the distribution of sand-rich sedimentary facies.

The source rock mechanical properties, permeability, mineral composition, and chemical characteristics are likely to directly affect the source supply and reservoir storage performance (Zhu et al., 2017). The carbonate rock weathering products are often transported to the sedimentary basin in the form of dissolution (Yang J. c., 1985; Pei et al., 2008). There are relatively few clastic particles and weaker supply capacity, which often cannot form large-scale sedimentary bodies. After undergoing diagenesis, the calcareous cementation becomes strong, with relatively dense reservoir, which is not conducive to high-quality reservoir development (Li et al., 2005; Feng et al., 2009). The granite rock erosion mainly consists of surface, gully, and collapse erosion, with a strong supply capacity and a high sand fraction (Ruan and Zhou, 1995), providing the conditions needed for high-quality reservoir formation.

7 Conclusion

Reconstructing source-to-sink systems in ancient continental basins is challenging due to the limitations and irreversibility of geological records. Based on a detailed description of the source-to-sink system of the second member of the Shahejie Formation in the Miaoxibe area, combined with geomorphological theory and the sedimentary backfilling method, this study has established a new method for reconstructing ancient continental basin source-to-sink system paleogeography. The source denudation evolution history in the study area was identified, and the source-to-sink system paleogeography of the second member of the Shahejie Formation was reconstructed.

This study provides a typical example for ancient source-to-sink system reconstruction in continental basins. This method can help to reconstruct near-source type source-to-sink system paleogeography in other ancient continental basins and further inform future basin and mountain tectonic evolution studies. Additionally, it can play a key role in guiding further denudation evolution history analysis in the source area. The reconstruction results have shown the source area paleogeographic evolution and provided information on sedimentary supply for the basin filling process. The findings are of considerable importance in paleo sedimentary environmental studies. The source-to-sink system elemental reconstruction, such as the source, transport pathways, and sedimentary facies, deepens our understanding of the sedimentary mechanisms and distribution law of sand-rich sedimentary systems such as deltas, provides a reference for

reservoir evaluation, and helps improve the success rate of reservoir prediction.

Data availability statement

The original contributions presented in the study are included in the article/Supplementary material, further inquiries can be directed to the corresponding author.

Author contributions

BF, YH, and HL contributed to conception and design of the study. TL organized the database. XD performed the statistical analysis. XH and XZ designed and conducted experiments. BF wrote the first draft of the manuscript. All authors contributed to the article and approved the submitted version.

Funding

This study was supported by the National Natural Science Foundation of China (Grant Nos 42272113 and 42272115).

References

- Allen, P. A. (2008). From landscapes into geological history. *Nature* 451, 274–276. doi:10.1038/nature06586
- Allen, P. A. (2005). Striking a chord. *Nature* 434, 961. doi:10.1038/434961a
- Amorosi, A., Maselli, V., and Trincardi, F. (2016). Onshore to offshore anatomy of a late quaternary source-to-sink system (po plain-adriatic sea, Italy). *Earth-Science Rev.* 153 (3), 212–237. doi:10.1016/j.earscirev.2015.10.010
- Anderson, J. B., Wallace, D. J., Simms, A. R., Rodriguez, A. B., and Taha, Z. P. (2016). Recycling sediments between source and sink during a eustatic cycle: systems of late quaternary northwestern gulf of Mexico basin. *Earth-Science Rev.* 153, 111–138. doi:10.1016/j.earscirev.2015.10.014
- Bai, W. H., Lv, X. M., Li, X. J., and Wei, W. (2002). The mode of paleo karstification and the fine reconstruction of the paleogeomorphology in the karst basin: taking ordovician karst in eastern ordos basin for example. *Geoscience* (03), 292–298. (in Chinese with English abstract).
- Du, X. F., Liu, H., Huang, X. B., Song, Z. Q., Xu, W., and Zhang, C. (2020). A near-shore clastic-carbonate mixing mode in a continental rift basin (early oligocene, eastern shijituo uplift, Bohai Bay Basin, China): sedimentology, reservoir characteristics and exploration practice. *J. Palaeogeogr.* 9 (04), 25–71. doi:10.1186/s42501-020-00074-w
- Feng, Z. G., Wang, S. J., Liu, X. M., Liu, X. M., and Luo, W. J. (2009). Impact of acid-insoluble residua of carbonate rocks on developing intensities of their weathering crusts. *ACTA Geol. SIN.* 83 (06), 885–893. (in Chinese with English abstract).
- Fielding, C. R., Ashworth, P. J., Best, J. L., Prokocki, E. W., and Smith, G. H. S. (2012). Tributary, distributary and other fluvial patterns: what really represents the norm in the continental rock record? *Sediment. Geol.* 261–262 (15), 15–32. doi:10.1016/j.sedgeo.2012.03.004
- Gao, S. (2005). Comments on the “NSF margins Program science Plans 2004”. *Mar. Geol. Quat. Geol.* (01), 119–123. (in Chinese with English abstract).
- Ge, J. W., Zhu, X. M., Lei, Y. C., and Yu, F. S. (2020). Tectono-sedimentary development in multiphase rift basins and a typical case study. *Earth Sci. Front.* (In Chinese with English abstract). doi:10.13745/j.esf.2020.5.9
- He, J., Shen, Z. G., Fang, S. X., Hou, F. H., Fu, S. T., Ma, Z. F., et al. (2007). Restoration of pre-carboniferous palaeokarst landform in central ordos basin. *Mar. Orig. Pet. Geol.* (02), 8–16. (in Chinese with English abstract).
- Helland, H. W., Somme, T. O., Martinsen, O. J., Lunt, I., and Thurmond, J. (2016). Deciphering earth’s natural hourglasses: perspectives on source-to-sink analysis. *J. Sediment. Res.* 86 (9), 1008–1033. doi:10.2110/jsr.2016.56
- Jiang, Z. L., Deng, H. W., Lin, H. X., and Wang, L. (2009). Methods and application of paleo-geomorphologies rebuilding an example of the second member of Shahejie

Acknowledgments

We gratefully acknowledge the Tianjin Branch of the China National Offshore Oil Corporation for providing data used in this study and permission to publish the results.

Conflict of interest

Author XD was employed by China National Offshore Oil Corporation. Authors XH and XZ were employed by Tianjin Branch of China National Offshore Oil Corporation.

The remaining authors declare that the research was conducted in the absence of any commercial or financial relationships that could be construed as a potential conflict of interest.

Publisher’s note

All claims expressed in this article are solely those of the authors and do not necessarily represent those of their affiliated organizations, or those of the publisher, the editors and the reviewers. Any product that may be evaluated in this article, or claim that may be made by its manufacturer, is not guaranteed or endorsed by the publisher.

Formation zhuangxi area, jiyang depression. *Geoscience* 23 (05), 865–871. (in Chinese with English abstract).

Jiang, Z. X. (2010). Studies of depositional systems and sequences stratigraphy: the present and the future. *Oil Gas Geol.* 31 (05), 535–541+514. (in Chinese with English abstract).

Li, C. R. (2015). Structure characteristics and favorable hydrocarbon exploration zone of Bodong Depression in Bohai Sea area. *Offshore oil.* 35 (04), 1–7.

Li, J. J. (1999). Memory of davisian theory of erosion cycle an peneplain: a centennial study in China. *J. Lanzhou Univ. Nat. Sci.* 03, 157–163. (in Chinese with English abstract).

Li, K., Zhao, X. K., Shen, Z. M., He, J. J., and Zhang, X. B. (2007). Application of trend met-hod in denudation recovery in the akekule lobe of tram basin. *Comput. Tech. Geophys. Geochem. Explor.* (05), 415–419+369. (in Chinese with English abstract).

Li, M. Q., Zhang, Z. R., Wang, Z. Y., Xu, J., and Qian, R. (2005). Tracing the pedogenic process of carbonate rocks in light of material and microfabric characteristics of clay and carbonate rocks: a case study of dashandong at guiyang rock-clay profile. *Earth Environ.* (04), 81–86. (in Chinese with English abstract).

Li, T. G., Cao, Q. Y., Li, A. C., and Qin, Y. S. (2003). Source to sink: sedimentation in the continental margins. *Adv. Earth Sci.* 18 (005), 713–721. (in Chinese with English abstract).

Li, Z. Y., Liu, Q. H., Zhu, H. T., Zhang, X. T., Li, M., and Zhao, Q. (2021). Compositional relationship between the source-to-sink segments and their sedimentary response to diverse geomorphology types in the intrabasin lower uplift of continental basins. *Mari ne Petroleum Geol.* 123, 104716. doi:10.1016/j.marpetgeo.2020.104716

Lin, C. S., Xia, Q. L., Shi, H. S., and Zhou, X. H. (2015). Carvedilol use is associated with reduced cancer risk: A nationwide population-based cohort study. *Earth Sci. Front.* 22 (01), 9–13. (in Chinese with English abstract). doi:10.1016/j.ijcard.2015.02.015

Lin, H. M., Liu, H., Wang, X. D., Qiu, X. W., Ju, Y. T., Meng, J., et al. (2022). Basin-filling processes and hydrocarbon source rock prediction of low-exploration degree areas in rift lacustrine basins: a case from the wenchang formation in low-exploration degree areas, northern Zhu I depression, pearl river mouth basin, E China. *J. Palaeogeogr.* 11 (2), 286–313. doi:10.1016/j.jop.2022.03.002

Liu, E. T., Chen, S., Y. D. T., Deng, Y., Wang, H., Jing, Z. H., et al. (2022). Detrital zircon geochronology and heavy mineral composition constraints on provenance evolution in the western pearl river mouth basin, northern south China sea: A source to sink approach. *Mar. Petroleum Geol.* 145, 105884. doi:10.1016/j.marpetgeo.2022.105884

- Liu, E. T., Wang, H., Feng, Y. X., Pan, S. Q., Jing, Z. H., Ma, Q. H., et al. (2020a). Sedimentary architecture and provenance analysis of a sublacustrine fan system in a half-graben rift depression of the South China Sea. *Sediment. Geol.* 409, 105781. doi:10.1016/j.sedgeo.2020.105781
- Liu, H., Loon, A. J., Xu, J., Tian, L. X., Du, X. F., Zhang, X. T., et al. (2020b). Relationships between tectonic activity and sedimentary source-to-sink system parameters in a lacustrine rift basin: A quantitative case study of the huanghekou depression Bohai Bay Basin, E China. *Basin Res.* 32 (4), 587–612. doi:10.1111/bre.12374
- Liu, P. B., Guan, D. Y., Wang, X., Li, C., Gao, S. K., and Zhang, H. Y. (2017). Study on quantitative characterization of ridge-fault coupling reservoir-controlling model in the Neogene of Bodong area, Bohai Sea, China. *J. Chengdu Univ. Technol. Sci. Technol. Ed.* 44 (04), 470–477. (in Chinese with English abstract).
- Liu, Q. H., Zhu, X. M., Li, S. L., Du, X. F., Li, H. Y., and Shi, W. L. (2016). System analysis in the shaleitain uplift. *Earth Sci.* 41 (11), 1935–1949. (in Chinese with English abstract).
- Liu, Q. H., Zhu, X. M., Li, S. L., Xu, C. G., Du, X. F., Li, H. Y., et al. (2017). Source-to-sink system of the steep slope fault in the Western Shaleitain Uplift. *Earth Sci.* 42 (11), 1883–1896. (in Chinese with English abstract).
- Liu, J. S., Lu, Y. C., and Qin, L. Z. (2019). Application of source to sink system analysis in large reservoir research: a case study of Huangang Formation, Central Inversion Belt, Xihu Depression. *Petroleum Geology & Experiment* 41 (03), 303–310. (in Chinese with English abstract).
- Martinsen, O. J., Tor Oftedal, S., William, H-H., Helland-Hansen, W., and Lunt, I. (2010). Source-to-sink systems on passive margins: theory and practice with an example from the Norwegian continental margin. *Geol. Soc. Lond. Pet. Geol. Conf. Ser.* 7, 913–920. doi:10.1144/0070913
- Martinsen, O. J., Lien, T., and Jackson, C. (2005). “Cretaceous and palaeogene turbidite systems in the North sea and Norwegian sea basins: source, staging area, and basin physiography controls on reservoir development,” in *Petroleum geology: North-west europe and global perspectives: Proceedings of the 6th petroleum geology conference*. Editors A. G. Dore and B. A. Vining (London: Geological Society), 1147–1164.
- Morehead, S. M. D., and Morehead, M. D. (1999). Estimating river-sediment discharge to the ocean: application to the eel margin, northern California. *Mar. Geol.* 154, 13–28. doi:10.1016/s0025-3227(98)00100-5
- Pei, J. H., Liang, M. Z., and Chen, Z. (2008). Classification of karst groundwater system and statistics of the main characteristic values in Southwest China karst mountain. *Carsologica Sin.* (01), 6–10. (in Chinese with English abstract).
- Romans, B. W., Castellort, S., Covault, J. A., Fildani, A., and Walsh, J. P. (2016). Environmental signal propagation in sedimentary systems across timescales. *Earth-Science Rev.* 153, 7–29. doi:10.1016/j.earscirev.2015.07.012
- Ruan, F. S., and Zhou, F. J. (1995). Several key problems about rebuilding vegetation on eroded granite slope. *Jouran soil water conservation* (02), 19–25. (in Chinese with English abstract).
- Sambrook Smith, G. H., Best, J. L., Ashworth, P. J., Fielding, C. R., Goodbred, S. L., and Prokocki, E. W. (2010). Fluvial form in modern continental sedimentary basins: distributive fluvial systems: comment. *Geology* 38 (12), e230. doi:10.1130/g31507c.1
- Shao, L. Y., Wang, X. T., Li, Y. N., and Liu, B. Q. (2019). Review on paleogeographic reconstruction of deep-time source-to-sink systems. *J. Paleogeogr. Chin. Ed.* 21 (1), 15. (in Chinese with English abstract).
- Sømme, T. O., Helland-Hansen, W., Martinsen, O., and Thurmond, J. B. (2009). Relationships between morphological and sedimentological parameters in source-to-sink systems: a basis for predicting semi-quantitative characteristics in subsurface systems. *Basin Res.* 21, 361–387. doi:10.1111/j.1365-2117.2009.00397.x
- Sømme, T. O., and Jackson, C. A. L. (2013). Source-to-sink analysis of ancient sedimentary systems using a subsurface case study from the more-trøndelag area of southern Norway: part 2 – sediment dispersal and forcing mechanisms. *Basin Res.* 25, 512–531. doi:10.1111/bre.12014
- South China Agricultural University (1980). *Foundation of geology*. Beijing: Agricultural Press, 121–123. (in Chinese).
- Syvitski, J. P. M., and Milliman, J. D. (2007). Geology, geography, and humans battle for dominance over the delivery of fluvial sediment to the coastal ocean. *J. Geol.* 115, 1–19. doi:10.1086/509246
- Tian, L. X., Liu, H., Niu, C. M., Du, X. F., Yang, B., Lan, X. D., et al. (2019). Development characteristics and controlling factor analysis of the neogene minghuazhen formation shallow water delta in huanghekou area, Bohai offshore basin. *J. Palaeogeogr.* 8 (3), 19–269. doi:10.1186/s42501-019-0032-8
- Walsh, J. P., Wiberg, P. L., Aalto, R., Nittrouer, C. A., and Kuehl, S. A. (2016). Source-to-sink research: economy of the earth’s surface and its strata. *Earth-Science Rev.* 153, 1–6. doi:10.1016/j.earscirev.2015.11.010
- Wang, P. X. (2009). Digging a time tunnel through the Earth system. *Sci. China Ser. D-Earth Sci.* 39 (10), 1313–1338. (in Chinese with English abstract).
- Weissmann, G. S., Hartley, A. J., Nichols, G. J., and Scuderi, L. A. (2010). Fluvial form in modern continental sedimentary basins distributive fluvial systems. *Geological Society of America* 31 (8), 39–42. doi:10.1130/G31507C.1
- Wu, K. Q., Wu, J. F., Liu, L. F., Huang, S. B., Li, C. R., and Du, H. Y. (2014). Tectonic transport and its impact on hydrocarbon accumulation: two cases of Bodong and Miaoqi Sag. *China Offshore Oil Gas* 26 (2), 6. (in Chinese with English abstract).
- Xia, R. Y., and Ma, Z. F. (1999). Ordovician paleoarts landform in Ordos Basin and gas enrichment characteristics. *Oil Gas Geol.* (02), 37–40. (in Chinese with English abstract).
- Xie, H., Zhou, D., Li, Y. P., Pang, X., Li, P. C., Chen, G. H., et al. (2014). Cenozoic tectonic subsidence in deep water sags in the Pearl River Mouth Basin, northern south China sea. *Tectonophysics* 615–616, 182–198. doi:10.1016/j.tecto.2014.01.010
- Xie, X. N., and Li, S. T. (1993). Characteristics of sequence stratigraphic analysis in terrestrial basin. *Geol. Sci. Technol. Inf.* (01), 22–26. (in Chinese with English abstract).
- Xu, C. G. (2013). Controlling sand principle of source-sink coupling in time and space in continental rift basin: basic idea, conceptual systems and controlling sand models. *China Off Shore Oil Gas* 25 (04), 1–11+21+88. (in Chinese with English abstract).
- Xu, C. G., and Du, X. F. (2017). Industrial application of source-to-sink theory in continental rift basin: a case study of Bohai sea area. *China Offshore Oil Gas* 29 (4), 9–18. (in Chinese with English abstract).
- Xu, C. G., Yang, H. F., Wang, D. Y., Zhao, D. J., and Wang, L. L. (2021). Formation conditions of neogene large-scale high-abundance lithologic reservoir in the laibei low uplift, Bohai sea, east China. *Petroleum Explor. Dev.* 48 (1), 15–29. doi:10.1016/s1876-3804(21)60002-2
- Yang J. C. J. C. (1985). *Geomorphology tutorial*. Beijing: Higher Education Press, 67–72. (in Chinese).
- Yang L. Z. L. Z. (1985). Distribution of subterranean rivers in south China. *Carsologica Sin.* (Z1), 98–106. (in Chinese with English abstract).
- Yu, B., Zhu, S. M., Zhu, Y., and Xie, H. (2013). Impacts of weathering on formation of gullied debris flow. *Bull. Soil Water Conservation* 33 (06), 51–56. (in Chinese with English abstract).
- Zeng, Z., Zhu, H., Mei, L., Du, J., Zeng, H., Xu, X., et al. (2019). Multilevel source-to-sink (S2S) subdivision and application of an ancient uplift system in south China sea: implications for further hydrocarbon exploration. *J. Petrol. Sci. Eng.* 181, 106220. doi:10.1016/j.petrol.2019.106220
- Zhang, C., Niu, C. M., Guan, D. Y., Liu, P. B., Zhou, X., and Xiao, J. Q. (2017). Polyethylene insert exchange Is crucial in debridement for acute periprosthetic infections following total knee arthroplasty. *Mar. Geol. Front.* 33 (01), 36–41. (in Chinese with English abstract). doi:10.1055/s-0036-1579667
- Zhao, G. X., Wang, Q. B., Yang, B., Wang, F. L., and Liu, F. (2017). LA-ICP-MS zircon U-Pb dating of Mesozoic granite in Miaoixbei Uplift, Bohai Sea area, and its geological significance. *Geol. Bull. China* 36 (7), 1204–1217. (in Chinese with English abstract).
- Zhao, Q., Zhu, H. T., Zhang, X. T., Liu, Q. H., Qiu, X. W., and Li, Min. (2021). Geomorphologic reconstruction of an uplift in a continental basin with a source-to-sink balance: an example from the huizhou-lufeng uplift, pearl river mouth basin, south China sea. *Mar. Petroleum Geol.* 128 (7176), 104984. doi:10.1016/j.marpetgeo.2021.104984
- Zhou, X. G., Huang, X. B., Song, Z. Q., Li, J., Liu, R., and Wang, Q. M. (2017). Provenance element control over the differential sedimentation of sand body in Ed3 of west Sag around Bozhong depression. *J. Northeast Petroleum Univ.* 41 (06), 120–121.
- Zhu, H. T., Xu, C. G., Zhu, X. M., Zeng, H. L., Jiang, Z. X., and Liu, K. Y. (2017). Advances of the source-to sink units and coupling model research in continental basin. *Earth Sci.* 42 (11), 20. (in Chinese with English abstract).
- Zhu, H. T., Yang, X. H., Liu, K. Y., and Zhou, X. (2014). Seismic-based sediment provenance analysis in continental lacustrine rift-basins: an example from the Bohai Bay Basin, China. *AAPG Bull.* 98 (10), 1995–2018. doi:10.1306/05081412159
- Zhu, H. T., Yang, X. H., Zhou, X. H., Li, J. P., Wang, D. Y., and Li, M. (2013). Sediment transport pathways characteristics of continental lacustrine basins based on 3-D seismic data: an example from Dongying Formation of western slop of Bozhong Sag. *Earth Science-Journal China Univ. Geosciences* 38 (01), 121–129. (in Chinese with English abstract).
- Zhu, X. (2020). *Characteristics of source-to-sink systems of depression-sinking sequence in the guantao Formation of the Bodong area, Bohai basin*. China University of Geosciences, 12–15. (in Chinese with English abstract).
- Zhu, X. M., Zhong, D. K., Yuan, X. J., Zhang, H. L., Zhu, S. F., Sun, H. T., et al. (2016). Development of sedimentary geology of petroliferous basins in China. *Petroleum Explor. Dev.* 43 (05), 890–901. (in Chinese with English abstract). doi:10.1016/s1876-3804(16)30107-0
- Zhu, X., Zhu, H. T., Zeng, H. L., and Yang, X. H. (2017). Subdivision, characteristics, and varieties of the source-to-sink systems of the modern lake erhai basin, yunnan province. *Earth Sci.* 42 (11), 2010–2024. (in Chinese with English abstract).